Selective adsorption of protein on polymer surfaces studied by soft X-ray photoemission electron microscopy

C. Morin, A. P. Hitchcock, R. M. Cornelius, J. L. Brash

BIMR, McMaster University, Hamilton, ON, Canada L8S 4M1

S.G. Urquhart

Dept. of Chemistry, University of Saskatchewan, SK, Canada S7N 5C9

A. Scholl and **A. Doran**

Advanced Light Source, Berkeley Lab, Berkeley, CA 94720

Abstract

X-ray photoemission electron microscopy (X-PEEM) using synchrotron radiation illumination in the C 1s, N 1s and O 1s regions has been used to characterize a phase segregated polystyrene/ polymethylmethacrylate (PS-PMMA) polymer thin film, and to map the adsorption of fibrinogen (a blood plasma protein) on this surface from both isotonic, buffered, and low ionic strength, unbuffered aqueous solutions at varying fibrinogen concentrations. The concentration dependence of the coverage correlates with independent, non-spatially resolved measurements using ^{125}I radiolabeled protein. At low concentrations (<0.1 mg/ml) of the buffered solution, adsorption of fibrinogen occurs with strong preference for PS domains. In contrast, adsorption from similar concentrations of unbuffered solution strongly prefers the interface of the PS and PMMA domains. Increasing the solution concentration up to 1 mg/ml of both buffered and unbuffered solutions leads progressively to full surface coverage (close-packed monolayer). These results demonstrate for the first time that X-PEEM with tunable soft X-rays has the sensitivity to locate and detect adsorbed proteins at the submonolayer level, while simultaneously detecting the spatial distribution of phases, and protein distribution relative to the phases, at the surface of an underlying microphase separated polymer substrate.

Keywords: photoemission electron microscopy, protein mapping, polystyrene, polymethylmethacrylate blend, polymer thin films, biomaterials

J. Electron Spectroscopy (submitted 30-Jun-03) (ICESS9 conference proceedings)
File: ICESS9-Fg-peem.doc Last changed: 20-Jun-03

Contact: Adam Hitchcock. aph@mcmaster.ca. V: 905 525-9140 x24749. F: 905 521-2773

1. INTRODUCTION

The biocompatibility of a material is believed to be related to the properties of the first protein layer adsorbed on contact with biological tissue or fluids. Initially adsorbed proteins are known to mediate the subsequent interactions of cells with the surface [1]. It is envisioned that novel surfaces that direct the biological healing process would have a well-defined array of bio-recognition sites designed to interact specifically with cells since many of the important functions of cells depend on type and orientation of molecules at their surfaces. In other cases, such as artificial materials used for blood contact, unfavorable aspects of first-layer protein adsorption can lead to coagulation, complement activation and other adverse responses. [2]. Thus, techniques which can map submonolayer amounts of adsorbed proteins at high spatial resolution, and thereby identify preferred sites of protein attachment on heterogeneous substrates, are of interest to assist development of biomaterials.

We are exploring the strengths and limitations of a number of soft X-ray microscopies for this purpose. Earlier we have shown that scanning transmission X-ray microscopy (STXM) can detect protein at near monolayer coverage adsorbed on structured polymers, even in the presence of a few micron overlayer of aqueous buffer [3]. While the ability to study wet systems is very attractive for approximating real world biomaterial-biological interfaces, the sensitivity to the actual polymer - protein interface is limited since the interface is only one part of the signal measured in a transmission experiment. The sampling depth of X-ray photoemission electron microscopy (X-PEEM) is ~10 nm, and thus X-PEEM, while a vacuum technique like XPS, should have significantly higher surface sensitivity than STXM and perhaps be better suited for this purpose. Here we report first explorations of X-PEEM for studies of protein adsorption.. The test substrate is a phase segregated blend of polystyrene (PS) and polymethyl methacrylate (PMMA), spun cast as a thin film on a Si wafer. We recently reported a detailed characterization of spun cast thin film PS/PMMA blends by AFM, PEEM and STXM [4]. The test protein for investigating selective adsorption on this surface is fibrinogen (Fg), a 340 kDa plasma protein that plays a central role in coagulation and thrombosis [5]. Fibrinogen adsorption from blood plasma is unusual in that more fibrinogen is adsorbed on most materials in a short exposure (10 s) than lengthy (1 h) contact times [6]. Also, more fibrinogen adsorbs from intermediate plasma dilutions than from either highly diluted or undiluted plasma. These phenomena, collectively

called the "Vroman effect" [5], are intriguing and suggest that fibrinogen molecules, once adsorbed, are eventually displaced from the surface by other adsorbing plasma proteins. While that concentration and exposure-time dependent behavior is specific for fibrinogen adsorption from the complex mixture of proteins present in plasma, it is interesting to measure adsorption from pure fibrinogen solutions as a reference point for the more complex, mixed protein plasma system, which will eventually be the target for study.

Measurements were performed using the electrostatic PEEM at the Advanced Light Source (ALS, Berkeley, CA) [7], and a magnetic PEEM at the Synchrotron Radiation Center (SRC, U. Wisconsin-Madison). Here we describe only the ALS results due to space limitations. We have recorded images, spectra, and image sequences in the C 1s, N 1s and O 1s regions on annealed PS-PMMA thin films both before and after exposure to fibrinogen. The protein adsorption was carried out from a phosphate buffer (pH 7.2) at concentrations from 0.005 mg/ml to 1 mg/ml, and from low ionic strength, un-buffered aqueous solutions at 0.05 and 0.1 mg/ml. Adsorption isotherm studies by ^{125}I-radiolabeling and atomic force microscopy (AFM) studies were also carried out. Together these results show that fibrinogen prefers the continuous PS domains when adsorbed from a buffer solution, but shows a strong preference for the PS/PMMA interface when adsorbed from non-buffered solution.

2. EXPERIMENTAL

2.1 Materials and methods

2.1.1 Substrate: PS (MW = 1.07 M, δ = 1.06) and PMMA (MW =312 K, δ = 1.01) were obtained from Polymer Source Inc. and were used without further purification. A 28:72 w/w PS/PMMA (1% by weight) toluene (Aldrich, 99.8% anhydrous) solution was spun cast (~50 µl drop, 4000 rpm, 30 s) onto clean 1x1 cm native oxide Si wafers (111) (Wafer World, Inc.), which had previously been degreased with trichloroethylene (Aldrich, +99.5% pure), acetone (Burdick & Jackson, HPLC grade), and methanol (Caledon), then rinsed under running milli-Q water. The PS:PMMA/Si substrates were annealed at 160°C for 8 hours in a vacuum oven with pressure ~10^{-2} torr. Non-contact mode AFM measurements of the PS:PMMA substrate and several Fg/PS:PMMA samples were made in the region of the Io normalization scratch. These showed the polymer film is 40-50 nm thick with 5-10 nm (RMS) corrugation in the PS:PMMA pattern. The adsorbed fibrinogen could not be reliably detected by our AFM measurements,

probably because of the softness of the polymer substrate, combined with a corrugation that is similar in size scale to the size of the adsorbed proteins.

2.1.2 Protein: Plasminogen-free human plasma fibrinogen (Calbiochem) was used as received. It is reported to be > 95% clottable by thrombin, and pure as judged by SDS-PAGE. Solutions for exposure to PS:PMMA were made at various concentrations in two different solvents, deionized water and phosphate buffer (Pierce, No. 28372, 0.1M sodium phosphate and 0.15M sodium chloride; when a pouch is dissolved in 500 ml deionized water, the pH is 7.2).

2.1 Methods

2.1. X-PEEM

X-PEEM of organic materials is challenging on account of potential problems with charging, field emission, and radiation damage. We have worked extensively to optimize our sample preparation, data acquisition, and data analysis procedures [8] to the point where we can measure many systems with minimal artifacts. Aspects important in this work are: keeping the PS:PMMA layer thin (<50 nm) and flat (~10 nm rms); using an internal reference (scratch through the film to expose Si for Io determination); use of a Ti filter to reduce second order radiation in C 1s region; use of beamline masks to decrease flux on the sample (at ALS beamline 7.3.1, the peak flux is ~10^{11} photons/s at 400 eV in a 30x30 μm spot). We have characterized the radiation damage rates for all three components [9]. As expected, PMMA is the most sensitive. Under the conditions used (masking to <~5 % of full flux), a 120 s measurement time leads to about 1/10^{th} of saturation damage. In order to have sufficient spectral definition and statistical precision, most of these measurements were made with a total exposure time ranging between 120-180 s, of which less than 50% of the time is used to acquire ~60 images, each with 1 s exposure, the remainder being overhead associated with data transfer and monochromator movement. With the masking conditions used the bending magnet beam is elliptically polarized with 70-80% right circularly polarized light. The electrostatic field at the sample was typically 9 kV/ mm, but this sometimes had to be reduced to as low as 8 kV/mm, in cases of mild charging. The intermediate voltage was then adjusted such that the resulting field-of-view was between 40 and 60 μm. The energy scales were calibrated from the known positions of the PS, PMMA and Fg structures [8,13] . The incident flux signal was taken from the region of a scratch through the

polymer film (see Fig. 1) for the C 1s and N 1s edges, and from the signal from a downstream Au mesh for the O 1s edge. The Io signals were corrected for the elemental photoabsorption response of Si or Au [10].

Image sequences (stacks) were prepared for analysis by: (1) energy calibration; (2) normalization to the elemental-corrected Io; (3) scaling the intensity to match to the elemental photoabsorption response of the substrate polymer, $C_5H_8O_{1.4}$ [10], based on the nominal 30:70 PS:PMMA stoichiometry. Assuming the work function is not strongly affected by the differing amounts of adsorbed protein, this approach should give an approximately quantitative analysis (percent composition of the region sampled) since the model spectra used in the analysis are placed on a linear absorption scale (signal per nm) which is set by matching to the elemental response. Component maps for PS, PMMA and Fg were then derived from these calibrated, normalized image sequences by either singular value decomposition (SVD)[11] or stack fit [12] fitting routines, within the aXis2000 X-ray microscopy analysis package [13]. Stack fit gave statistically better fits than SVD since it incorporates an additional constant term which accommodates uncorrected backgrounds such as those from camera offsets, and possibly some long escape depth signal from the underlying Si wafer. For the C 1s and O 1s edges, fits were made to 3 components (PS, PMMA, Fg) while for the N 1s edge, the fit was made only to 2 components (PS, Fg) since the PS and PMMA are indistinguishable in this energy region.

2.2.2 Protein exposure

For X-PEEM the Fg/PS:PMMA samples were prepared by 10 min. incubation of the PS:PMMA substrate for in ~2 ml of Fg solution contained in a Fisher multiwell plate (1 cm diameter wells), followed by continuously diluting the overlayer solution with running deionized water for ~3-5 minutes. The Fg/PS:PMMA substrate was then removed from the well. This rinsing method was used to avoid depositing protein or buffer salts from the air-solution interface.

2.2.3 Experiments with radiolabeled fibrinogen

Fibrinogen was labeled with ^{125}I (ICN Biomedicals, Mississauga, Ontario, Canada) using the iodogen technique [14], a standard protocol for radioiodination of proteins by IODO-GEN® (Pierce Chemical Company, Rockford, IL) [15]. The labeled protein was dialyzed overnight against isotonic Tris buffer to remove unbound radioactive iodide. Trichloroacetic acid

precipitation [16] of protein solutions before and after completion of the experiments confirmed that > 99% of the ^{125}I remained bound to the protein. The adsorption experiments were carried out in phosphate buffered saline (pH 7.2) with 4 repeats and in milli Q-water (3 repeats), also for 10 minute exposures. For the radio-labeling experiments the samples were rinsed statically for 2.5 minutes in a similar volume of buffer solution, and three times more for 2.5 minutes each in milli-Q water. Adsorbed amounts were calculated as described earlier[17]. For the blend surface, it was demonstrated that batch rinsing and continuous rinsing gave the same adsorption isotherm.

3. RESULTS

3.1 PS:PMMA substrate

Fig. 1 presents selected energy images and selected region C 1s spectra measured with X-PEEM. The raw images show the PS:PMMA phase segregated pattern only at the energies of strong PS (285.1 eV) and strong PMMA (288.5 eV) absorption peaks, with contrast inversion. Fig. 1 also presents PS and PMMA component maps derived from singular value decomposition (SVD) analysis [11] of the C 1s image sequence and a color composite map. X-ray damage to PMMA [9] results in loss of C=O bonds, leading to intensity loss at 288.2 eV, and formation of C=C bonds, leading to intensity gain at 285 eV. The C 1s image sequence for PS:PMMA was measured for 140 s, about the time for ~10% of saturation damage, and thus should have barely detectible signal at 285 eV. In fact the PMMA domains do exhibit a significant 285.1 eV signal. In this particular example very little of the 285 eV signal is from radiation damage; the majority is associated with PS micro-domains embedded in the PMMA macro-domains [4] which, to date, are an unavoidable feature of our sample preparation. Based on analysis of the C 1s spectrum averaged over large areas, the composition in the depth sampled by X-PEEM (estimated as 5-10 nm) is 57(2):43(2) w/w, significantly enriched in PS relative to the formulation, as found earlier [4].

Table 1 reports the advancing water contact angles for the pure PS, pure PMMA and the PS:PMMA blend surface. Pure PS is more hydrophobic than pure PMMA. The water contact angle for PS:PMMA falls at an intermediate value, one that is consistent with the actual 57:43 surface composition, as opposed to the 28:72 formulation.

3.2 I_{125}-Fg on PS:PMMA adsorption isotherms

Fig. 2 shows isotherms for adsorption of ^{125}I-labeled Fg from phosphate buffer to pure PS, to pure PMMA and tp the PS:PMMA blend surface. Across the entire concentration range there is a significantly greater amount of Fg adsorbed to the PS than to the PMMA, while the blend surface adsorbs an intermediate amount. The adsorbed amounts at the higher concentrations are in the range of close-packed monolayers. The higher amounts on PS occur not just at monolayer saturation but also in the low concentration regime. This suggests that, for the 10 minute exposure time used, the adsorbed amount on the 3 different surfaces reflects relative binding affinities rather than any kinetic effect. The adsorption behavior as monitored by ^{125}I-labeling, is also sensitive to the ionic strength of the adsorbing solution. As shown in the insert to Fig. 2, the slope of the isotherm in the <0.1 mg/mL regime for Fg adsorption from buffer is ~1.5 x as steep as that for Fg adsorption from water. For adsorption from buffer these results suggest that for the PS:PMMA blend, Fg will adsorb preferentially to PS rather than to PMMA domains. However, the data also indicate there is no preference when the solvent is water, at least for concentrations up to 50 μg/ml.

3.3 X-PEEM of Fg/ PS:PMMA

3.3.1 Reference spectra

Fig. 3 shows the NEXAFS spectra of pure PS, PMMA and Fg spun cast thin films in the C 1s, N 1s and O 1s regions, recorded with X-PEEM. The dotted lines are the expected elemental responses [10]. All 3 materials exhibit distinct C 1s spectra. The Fg and PMMA spectra are each dominated by C 1s (C=O) → $\pi^*_{C=O}$ transitions. However the $\pi^*_{C=O}$ peak in Fg occurs 0.3 eV below the $\pi^*_{C=O}$ peak in PMMA since the carbonyl carbon is in a less electronegative environment (CONH vs. COOR). Due to the small size of this shift and the otherwise similar nature of the Fg and PMMA C 1s spectra, accurate energy calibration is essential for reliable analysis. Addition of signal from the N 1s and O 1s edges significantly enhances the ability of NEXAFS to differentiate these species. Only Fg has a N 1s spectrum. It has the characteristic N 1s → π^*_{CONH} transition at 401.2 eV, as found in other proteins and peptides [18,19]. At the O1s edge, PMMA and Fg each are dominated by O 1s → $\pi^*_{C=O}$ transitions at 531.6 eV, but PMMA has an extra transition at 535.5 eV arising from O1s (O-CH_3) → $\pi^*_{C=O}$ transitions, specific to esters.

3.3.2 Fg (buffer)/PS:PMMA

Fig 4. presents stack fit analysis of the C 1s image sequence for Fg adsorption from 0.05 mg/ml buffer solution. In the composite map (a), the continuous PS domains are purple rather than red, whereas the PMMA domains are pure green. This indicates that Fg sits preferentially on the PS domains. The Fg component map (d) provides the same information. Note that the smallest regions with detectable protein signal are about 200 nm, ~ 4 times the size of a single protein [20], indicating that with slightly improved signal it may be possible to map single protein molecules with X-PEEM. The right hand panel of Fig 3 presents curve fits to spectra extracted from regions of strong PS, PMMA and Fg signals. The extracted regions are indicated by the color outline regions in the grayscale component maps (b-d). The numerical results for fits to spectra of similarly selected PS-rich, PMMA-rich and Fg-rich regions for all four Fg(buffer)/PS:PMMA systems studied are presented in **Table 2**. For the 0.05 mg/ml Fg(buffer) system quantitative spectral analysis indicates that the centre of the PS domains contain over ~20 % Fg. Similarly, the spectrum of pixels with strong Fg components is analyzed to contain 45% PS and negligible amounts of PMMA. Finally, the centre of the PMMA domains is dominated by PMMA (70%) with the remaining signal mostly PS (21%), probably associated with micro-domain PS [4], although possibly also reflecting some radiation damage.

Fig 5. shows the C1s spectra extracted for pixels of high PS (left) and high Fg (right), for four concentrations between 0.005 mg/ml and 1.0 mg/ml of Fg(buffer). For the lowest protein concentration, the high PS region spectrum is virtually identical to that of pure PS, while for the same concentration, the high-Fg has a strong PS signature, consistent with its location on the PS domains., as shown by the mapping in **Fig 4.** As the protein concentration increases to 1.0 mg/ml, the high PS spectra show an increasing 288.2 eV $\pi^*_{C=O}$ peak from the Fg. For adsorption from a 1.0 mg/ml solution, the Fg signal is stronger than that for PS. As expected, the C 1s spectrum of high-Fg pixels becomes progressively more like pure Fg as the Fg concentration increases. Also, the high-Fg pixels are spread over increasingly large areas as the concentration increases, and the high-Fg location changes from "on PS-only" for the two lowest concentrations, to nearly full surface coverage at 1.0 mg/ml. The corresponding results for the PMMA-rich pixels support the conclusion of PS-preference at low coverage, and whole-surface coverage at high concentration.

However the plots are not shown since the high-PMMA spectra for exposure from low concentration Fg(buffer) solutions are distorted by radiation damage.

3.3.3 Fg (water)/PS:PMMA

Fig. 6 presents color composite maps derived by stack fit analysis of C 1s, N 1s and O 1s image sequences recorded for Fg adsorption from 0.05 mg/ml unbuffered, low ionic strength aqueous solution. In contrast to the corresponding isotonic buffered system (Fig. 4), the C 1s composite map (6a), shows that the Fg is adsorbed preferentially at the boundary of the PS and PMMA domains. This is supported by the O 1s and particularly the N 1s composite maps, which also show the Fg signal preferentially at the PS:PMMA interface. While the color coded composite maps give the spatial registry of the components, one can legitimately ask: "is this simply artistry?". To demonstrate the origin of these signals, the lower three panels in Fig. 6 are the spectra extracted from the PS-rich, PMMA-rich, and Fg-rich pixels which are taken from the color coded regions in the insets in the spectral plots. These regions were selected by defining a region of interest through a threshold masking procedure applied to the component maps. Without a doubt, the interface regions show a strong enhancement in the Fg signatures at each core edge, while the PMMA domains show negligible Fg signal. The curve fit analysis of these results are summarized in **table 3**, along with the results from a similar analysis of C 1s, N 1s, and O 1s image sequences for a 0.1 mg/ml Fg/PS:PMMA sample.

4. DISCUSSION AND SUMMARY

This work provides the first demonstration that X-PEEM can map selective adsorption of a protein on the different domains of a chemically heterogeneous polymer surface with a spatial resolution better than 0.1 micron. The data from X-PEEM is shown to provide mapping information that is complementary to the total surface concentration data obtained from radiolabeled protein experiments.

Perhaps the most striking result from this study is that at low protein concentration and low ionic strength in unbuffered medium, the protein adsorbs preferentially at the interface between the PS and PMMA domains. This observation is not unexpected from the point of view that proteins are highly surface active and "prefer" the interfacial environment to any other. In this case the interface is among three "phases" (water, PS, PMMA) instead of the more usual two.

Presumably attachment at this location is the strongest, and results in the lowest free energy of the system.

The interdomainal location is not preferred when the protein is in isotonic buffer at pH 7.2. Instead, adsorption occurs predominantly on the PS domains. Differences in the behavior of fibrinogen in these two media may be expected on the basis of a difference in net charge due both to different pH in relation to the isoelectric point (pI=5.5 for fibrinogen) and to charge screening effects at high ionic strength. However, since there are no formal charges on either PMMA or PS, charge effects at low surface coverage should be minimal. Fibrinogen is less soluble in water than in isotonic buffer and thus would be expected to adsorb more extensively from water. However, the similarity of the isotherms at low coverage (Figure 2) suggests that the effects of any small solubility difference may be negligible: indeed, the ^{125}I radio-labeling shows that adsorption is lower from water than from buffer. For the moment there is no obvious reason for the difference in adsorption patterns from the two media. It may be speculated that there are conformational effects that play a role in these phenomena.

The present results suggest that, for the 10 min exposure employed, thermodynamic factors (binding affinity) rather than kinetic factors control adsorption. It would be interesting to extend the measurements to shorter exposure times to see if the site preference remains the same or changes in a kinetic-controlled regime.

Using hydrophobicity gradient surfaces, it has been shown convincingly that proteins adsorb more extensively and with greater affinity to hydrophobic compared to hydrophilic surfaces [21,22]. It has also been shown by Rapoza et al [14] that Fg in isotonic buffer adsorbs with greater affinity to hydrophobic compared to hydrophilic surfaces. They found that glassy, rigid polymers (such as PS) showed relatively high fibrinogen adsorption, regardless of whether the polymer was hydrophobic or hydrophilic. However, the binding strength (as measured by elutability) was much lower on hydrophilic polymers and oxygen-containing hydrophobic polymers (such as PMMA). Our results are in accord with these findings in that our radiolabeling data show more extensive adsorption of Fg on PS than on PMMA, and our X-PEEM data show preferential adsorption to the PS domains in the blends at low coverage.

This work has shown that X-PEEM can simultaneously map the chemical structure of a thin film polymer support and sub-monolayer amounts of adsorbed protein. We believe that this approach to the study of protein adsorption will have important applications in the design and

surface characterization of biomaterials, e.g. in sub-micron spatial patterning of proteins at the biological - biomaterial interface. These methods may also be useful in other applications where spatial selectivity of adsorption is important (e.g. protein separation and purification). Future work will explore extension of the technique to competitive adsorption in multi-protein systems (eg plasma, tear fluid). For these systems, it is anticipated that heavy atom labeling will be required to differentiate proteins one from another.

ACKNOWLEDGEMENTS

This research is supported by Natural Science and Engineering Research Council (NSERC, Canada) and the Canada Research Chair programs. X-ray microscopy was carried out using PEEM2 at the ALS (supported by DoE under contract DE-AC03-76SF00098) and the Canadian PEEM at SRC (supported by NSF under award DMR-0084402). The Canadian PEEM was funded by NSERC. Cynthia Morin acknowledges the support of an ALS graduate fellowship during which time most of this work was performed.

REFERENCES

1. D.G. Castner and B.D. Ratner, Surface Science 500 (2002) 28.
2. M. Tirrell, E. Kokkoli, and M. Biesalski, Surface Science 500 (2002) 61.
3. A.P. Hitchcock, C. Morin, Y.M. Heng, R.M. Cornelius and J.L. Brash, J. Biomaterials Science, Polymer Ed. 13 (2002) 919.
4. C. Morin, H. Ikeura-Sekiguchi, T. Tyliszczak, R. Cornelius, J.L. Brash, A.P. Hitchcock A. Scholl, F. Nolting, G. Appel, A. D. Winesett, K. Kaznacheyev and H. Ade, *J. Electron Spectrosc* 121 (2001) 203.
5. A. L. Bloom and P. T. Thomas (Eds), *Haemostasis and Thrombosis.* Churchill Livingstone, New York (1987)
6. S. M. Slack and T. A. Horbett,, J. Biomater. Sci. Polymer Edn . 2 (1991) 227.
7. S. Anders, H.A. Padmore, R.M. Duarte, T. Renner, T. Stammler, A. Scholl, M.R. Scheinfein, J. Stöhr, L. Séve and B. Sinkovic, Rev. Sci. Inst. 70 (1999) 3973.
8. C. Morin, A.P. Hitchcock, H. Ikeura-Sekiguchi, A. Scholl, A, Doran, K. Kaznacheyev, 2001 ALS Compendium, LBNL publication (2002).
9. C. Morin, A.P. Hitchcock, K. Kaznatcheev, A. Doran and A. Scholl, in preparation
10. B.L. Henke, E.M. Gullikson, and J.C. Davis, At. Data Nucl. Data Tables 54 (1993) 181.

11. I.N. Koprinarov, A.P. Hitchcock, C. McCrory and R.F. Childs, J. Phys. Chem. B 106 (2002) 5358.
12. A.P. Hitchcock et al, Chemical Record (in preparation)
13. 30. aXis2000 is a freeware program written in Interactive Data Language (IDL), and available from http://unicorn.mcmaster.ca/aXis2000.html.
14. R.J. Rapoza and T.A. Horbett, J. Biomed. Mat. Res., 24 (1990) 1263.
15. Pierce Chemical Company, IODO-GEN Iodination Reagent, 1993.
16. E. Regoeczi, *Iodine-Labeled Plasma Proteins*, Vol. 1, (CRC Press, Boca Raton, FL, 1984)
17. B. M. C. Chan and J. L. Brash, J. Colloid Interface Sci., 82 (1981) 217
18. B.W. Loo, Jr., I.M. Sauerwald, A.P. Hitchcock and S.S. Rothman, J. Microscopy 204 (2001) 69.
19. M. Gordon, G. Cooper, T. Araki, C. Morin, C. C. Turci, K. Kaznatcheev, and A. P. Hitchcock, J. Phys. Chem A (2003) in press.
20. J. H. Brown, N. Volkmann, G. Jun, A. H. Henschen-Edman, and C. Cohen, Proc.Nat. Acad. Sci USA 97 (2000) 85
21. H. Elwing, A. Askendal, B. Ivarsson, U. Nilsson, S. Welin, I. Lundstrom. Am. Chem. Soc. Symp. Ser. 343, (1987) 468.
22. H. Elwing, S. Welin, A. Askendal, U. Nilsson, I. Lundstrom. J. Colloid Interface Sci. 119 (1987) 203.
23. D.K. Han, G.H. Ryu, K.D. Park, S.Y. Jeong, Y. H. Kim, and B.G. Min, J. Biomater. Sci. Polymer Edn. 4 (1993) 401.
24. R. G. Craig, G. C. Berry, F. A. Peyton; J. Phys. Chem., 64 (1960) 541

Table 1 Advancing water contact angle [(a)] for PS, PMMA and PS:PMMA

Sample	Angle on sample[(b)]	Literature
PS	77.5(4)	86[(c)]
PS:PMMA	74.9(8)	-
PMMA	70.7(3)	62-73[(d)]

(a) Advancing water contact angles were measured using the sessile drop method. Milli-Q water and a Ramé-Hart (Mountain Lakes, NJ) NRL goniometer were used for these measurements.
(b) error in last digit is based on spread of two measurements.
(c) ref 23
(d) ref 24

Table 2 Composition[(a)] of selected PS-rich, PMMA-rich and Fg-rich regions from analysis of C 1s image sequences of a PS/PMMA sample exposed for 10 m to phosphate-buffered Fg solution

A) 0.005 mg/ml

	Relative amounts (%)[(b)]			
Region masked	PS	PMMA	Fg	Normalization
PS	**87**	11	1	1.43
PMMA	28	**64**	8	1.38
Fg	54	5	**41**	1.59

B) 0.05 mg/ml

	Relative amounts (%)[(b)]			
Region masked	PS	PMMA	Fg	Normalization
PS	**79**	2	19	1.89
PMMA	21	**70**	9	2.32
Fg	45	1	**55**	1.71

C) 0.1 mg/ml

	Relative amounts (%)[(b)]			
Region masked	PS	PMMA	Fg	Normalization
PS	**58**	6	35	1.61
PMMA	21	**68**	0	1.39
Fg	28	11	**61**	1.75

D) 1.0 mg/ml

	Relative amounts (%)[(b)]			
Region masked	PS	PMMA	Fg	Normalization
PS	**37**	28	35	1.47
PMMA	25	**63**	12	1.47
Fg	25	31	**43**	1.49

(a) The values in the table are percentages derived from the average from selected regions (see Fig. 4, for the case of 0.05 mg/ml Fg exposure) of the PS, PMMA and Fg component maps reported by a 3-component stack fit analysis (C1s, O1s) or a 2-component stack fit analysis (N1s). If the work function of the various parts of the surface, and different systems is the same, the normalization of the intensity of the image sequences (see text) should result in summation of the coefficients to unity. Deviations of that sum from unity indicate systematic errors such as incorrect intensity normalization as well as statistical errors. The normalization factor (right most column) gives a sense of the size of errors.

(b) standard deviations of the curve fits to the selected region spectra are between 5×10^{-5} and 5×10^{-4}.

Table 3 Composition[(a)] of selected PS-rich, PMMA-rich and Fg-rich regions from analysis of C1s, N1s, and O1s image sequences of a Fg(water)/PS:PMMA samples

A) 0.05 mg/ml Fg (water)

C 1s

	Relative amounts (%)[(b)]			
Region masked	PS	PMMA	Fg	Normalization
PS	**77**	23	0	1.79
PMMA	9	**72**	19	1.72
Fg	25	31	**44**	1.92

N 1s [(c)]

	Relative amounts (%)[(b)]			
Region masked	PS	PMMA	Fg	Normalization
PS/PMMA	-	**91**	9	0.85
Fg	-	29	**71**	1.03

O 1s

	Relative amounts (%)[(b)]			
Region masked	PS fit[(b)]	PMMA fit[(b)]	Fg fit[(b)]	Normalization
PS	**30**	0	70	1.02
PMMA	79	**17**	4	0.72
Fg	0	19	**81**	0.82

B) 0.1 mg/ml Fg (water)

C 1s

	Relative amounts (%)[(b)]			
Region masked	PS	PMMA	Fg	Normalization
PS	**91**	0	9	1.44
PMMA	14	**78**	7	1.01
Fg	67	13	**21**	1.59

N 1s [(c)]

	Relative amounts (%)[(b)]			
Region masked	PS	PMMA	Fg	Normalization
PS/PMMA	-	**91**	9	1.03
Fg	-	36	**64**	1.06

O 1s

	Relative amounts (%)[(b)]			
Region masked	PS	PMMA	Fg	Normalization
PS	**32**	0	68	0.88
PMMA	63	**32**	5	0.68
Fg	19	9	**72**	0.93

(a) see footnote (a) of table 2.(b) see footnote (b) of table 2

(c) N 1s image sequence was only fit to 2 components as PS and PMMA are indistinguishable at this edge

Figure Captions

FIGURE 1. (a) X-PEEM images at 283, 285.1, 288.4 and 290 eV, 4 of 40 images in the C 1s region of an annealed 28:72 w/w PS:PMMA blend thin film spun cast on native oxide Si (note the actual average surface composition is 57:43 - see text). (b) Spectra from the indicated spots. (c,d) Component maps of PS and PMMA derived by singular value decomposition of the C 1s image sequence (e) color coded composite map (R=PS, G=PMMA).

FIGURE 2. Isotherms for adsorption of ^{125}I -labeled Fg from phosphate buffer pH 7.2 to pure PS, pure PMMA and the PS:PMMA blend surface. The inset compares the isotherms at low concentration from phosphate buffer and water.

FIGURE 3. C 1s, N 1s and O 1s NEXAFS spectra of PS, PMMA and Fg recorded as pure materials with X-PEEM. The dashed lines indicate the elemental response [10]. Offsets are used for clarity.

FIGURE 4. (a) Composite map (R=PS, G=PMMA, B=Fg) derived from component maps extracted by stack fit analysis of a C 1s image sequence for fibrinogen (0.05 mg/ml in buffer) adsorbed on the PS:PMMA blend surface. (b-d) Component maps indicating the extracted regions of high PS, high PMMA and high Fg signals. (e-g) Curve fits of the extracted spectra.

FIGURE 5. (a) spectra from high-PS pixels of the PS component maps generated from stack fit analysis of C1s image sequences recorded for fibrinogen (0.005, 0.01, 0.05 and 1.0 mg/ml in buffer) adsorbed on the PS:PMMA blend surface. (b) same for spectra of high-Fg pixels of the Fg component map.

FIGURE 6: (a) Color composite map and high-PS, high-PMMA and high-Fg extracted spectra derived from C1s image sequence recorded for 0.05 mg/ml Fg (water). The insets in the spectral plot indicates the region from which the spectrum was extracted. (b) Same for N 1s image sequence. In this case only a 2-component fit was carried out, (c) Same for O 1s image sequence.

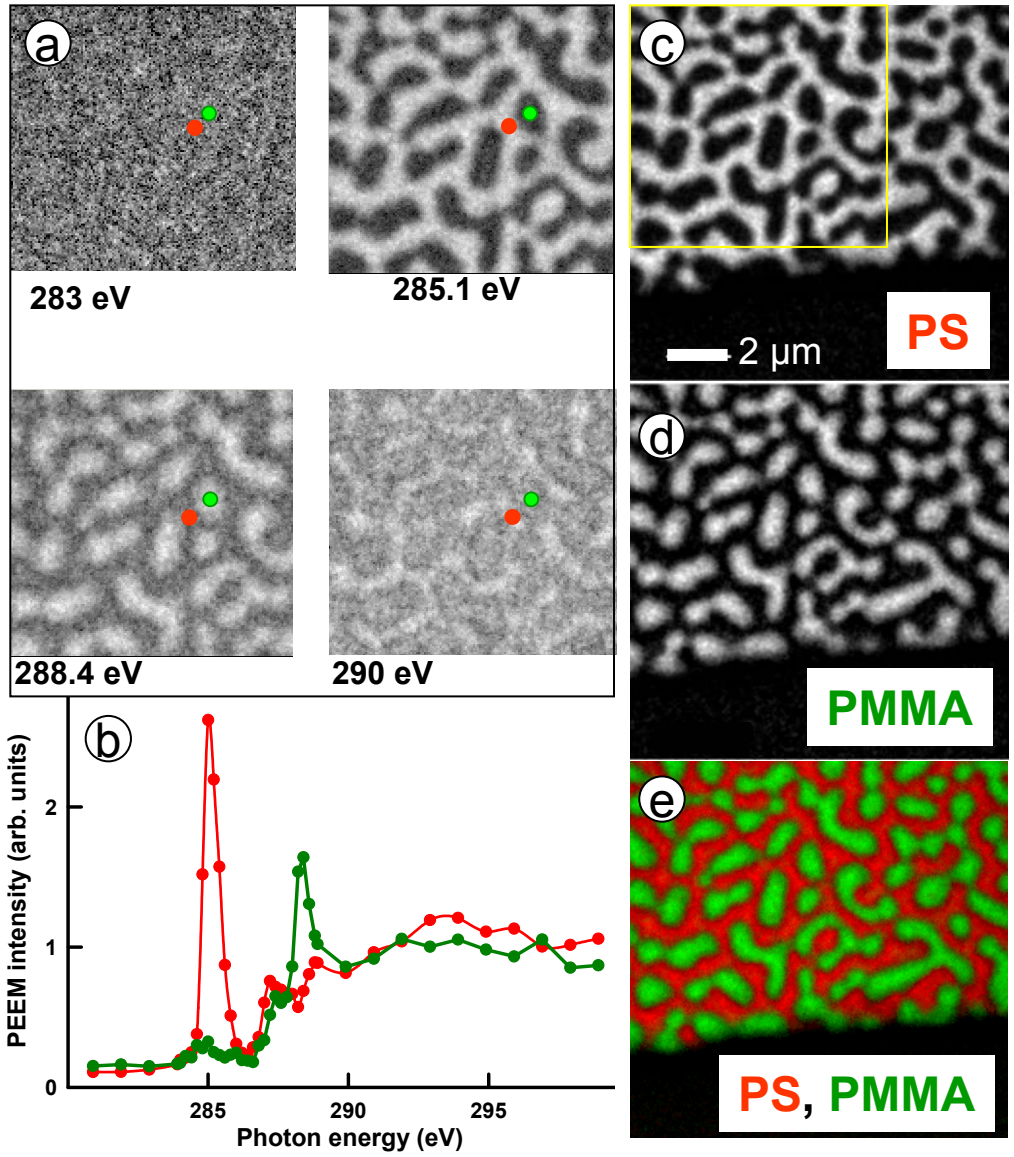

Morin et al. (J. El. Spec.) 18-jun-03

Fig 1

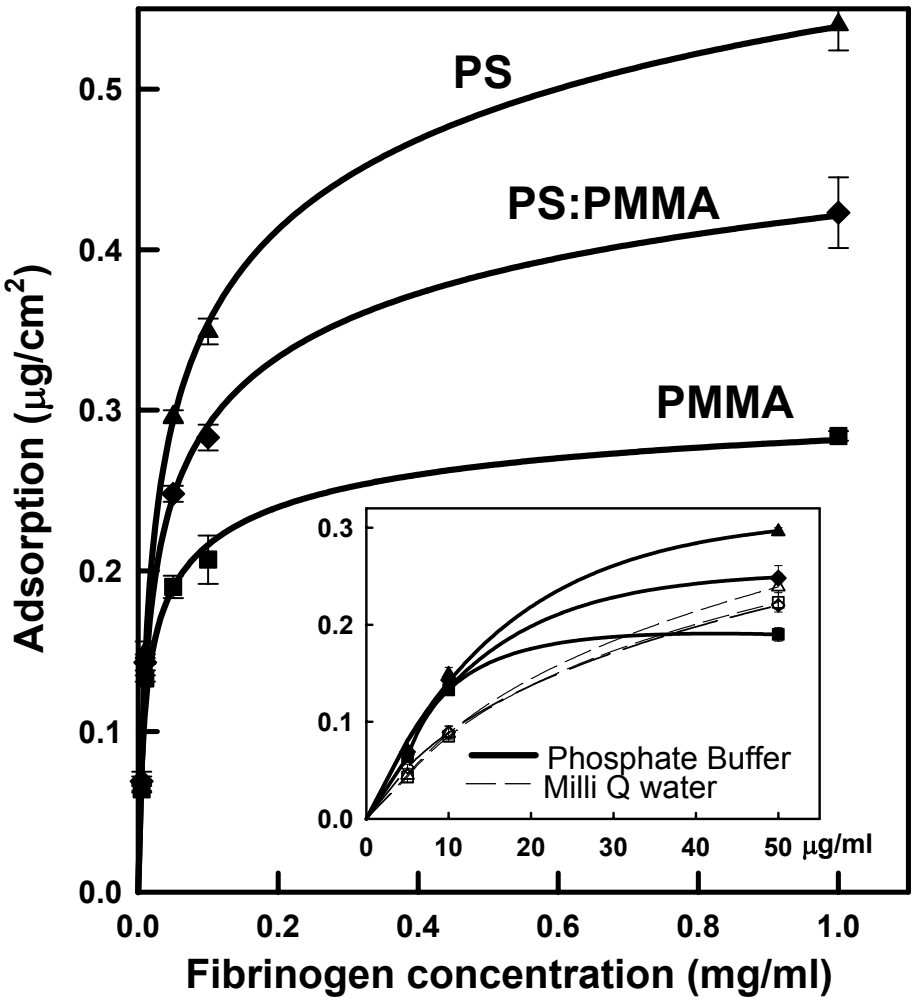
PS
PS:PMMA
PMMA
Adsorption (μg/cm²)
Fibrinogen concentration (mg/ml)
0.0
0.1
0.2
0.3
0.4
0.5
0.6
0.8
1.0
Phosphate Buffer
Milli Q water
0
10
20
30
40
50 μg/ml

Fig 2

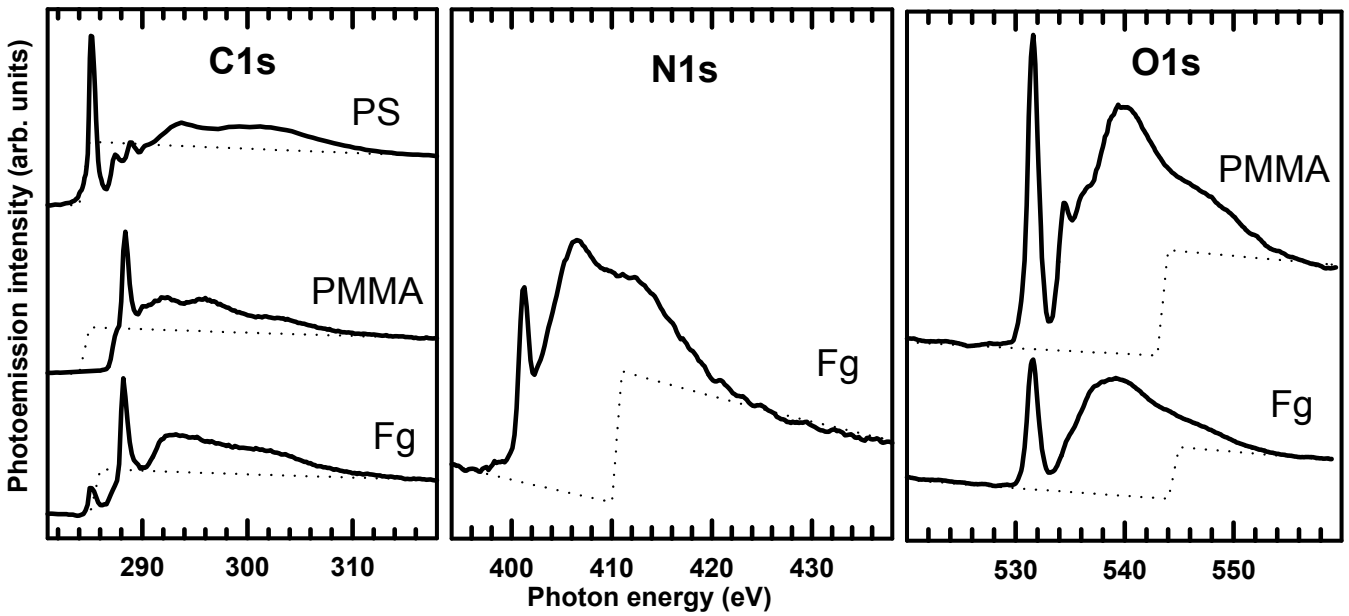
C1s
PS
PMMA
Fg
N1s
Fg
O1s
PMMA
Fg
Photoemission intensity (arb. units)
290
300
310
400
410
420
430
530
540
550
Photon energy (eV)

Fig 3

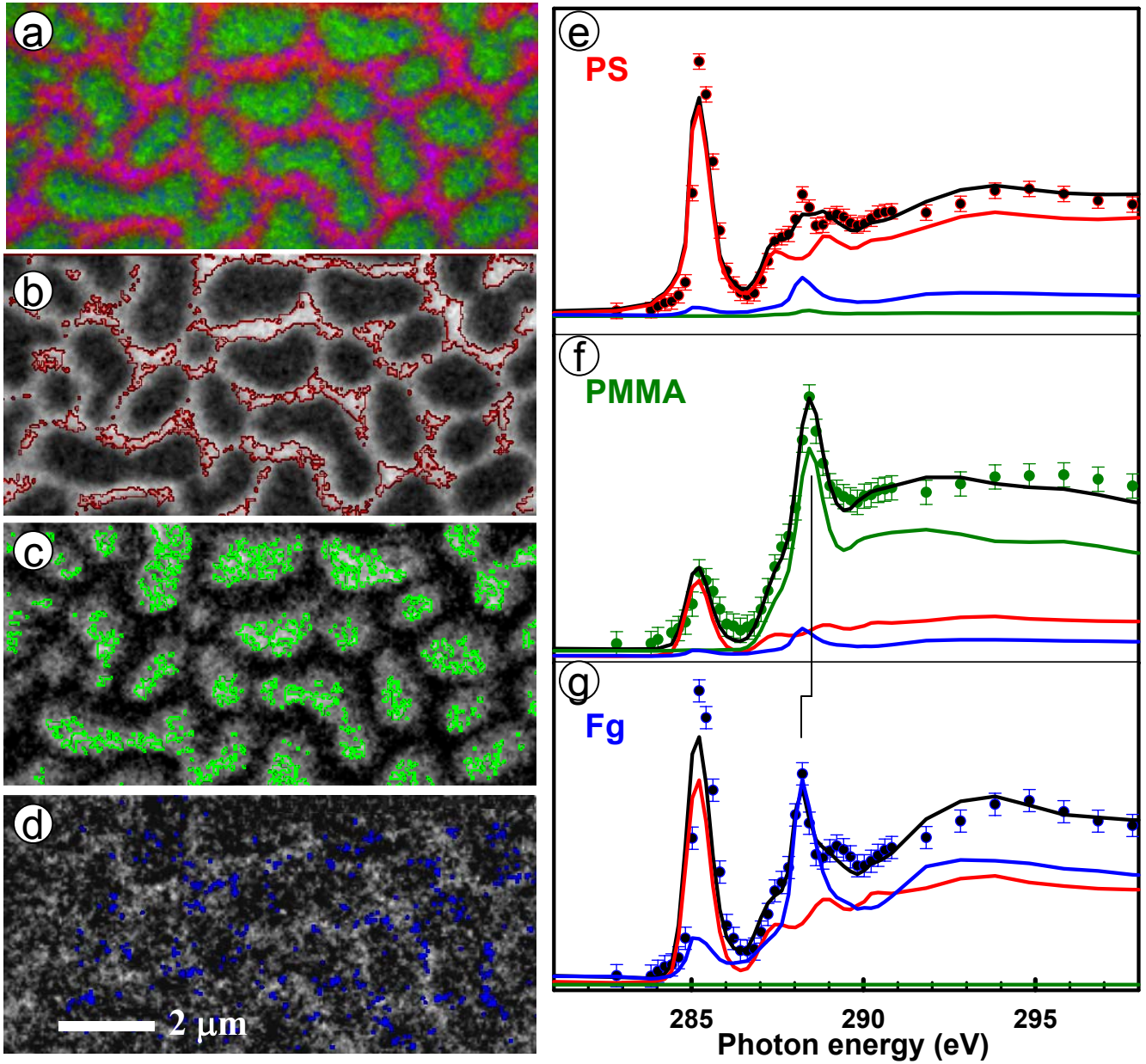

Fig 4

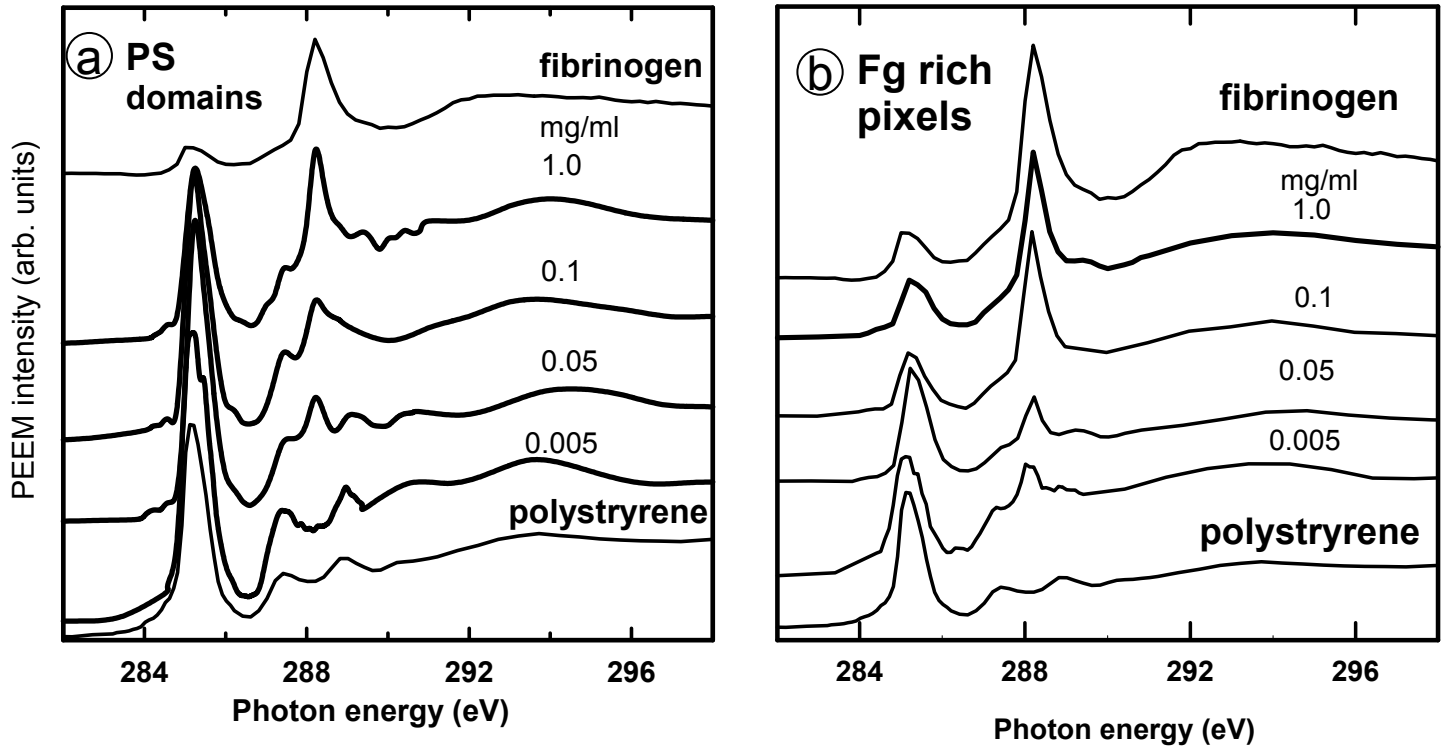
ⓐ PS
domains
fibrinogen
mg/ml
1.0
0.1
0.05
0.005
polystryrene
PEEM intensity (arb. units)
284
288
292
296
Photon energy (eV)
ⓑ Fg rich
pixels
fibrinogen
mg/ml
1.0
0.1
0.05
0.005
polystryrene
284
288
292
296
Photon energy (eV)

Fig 5

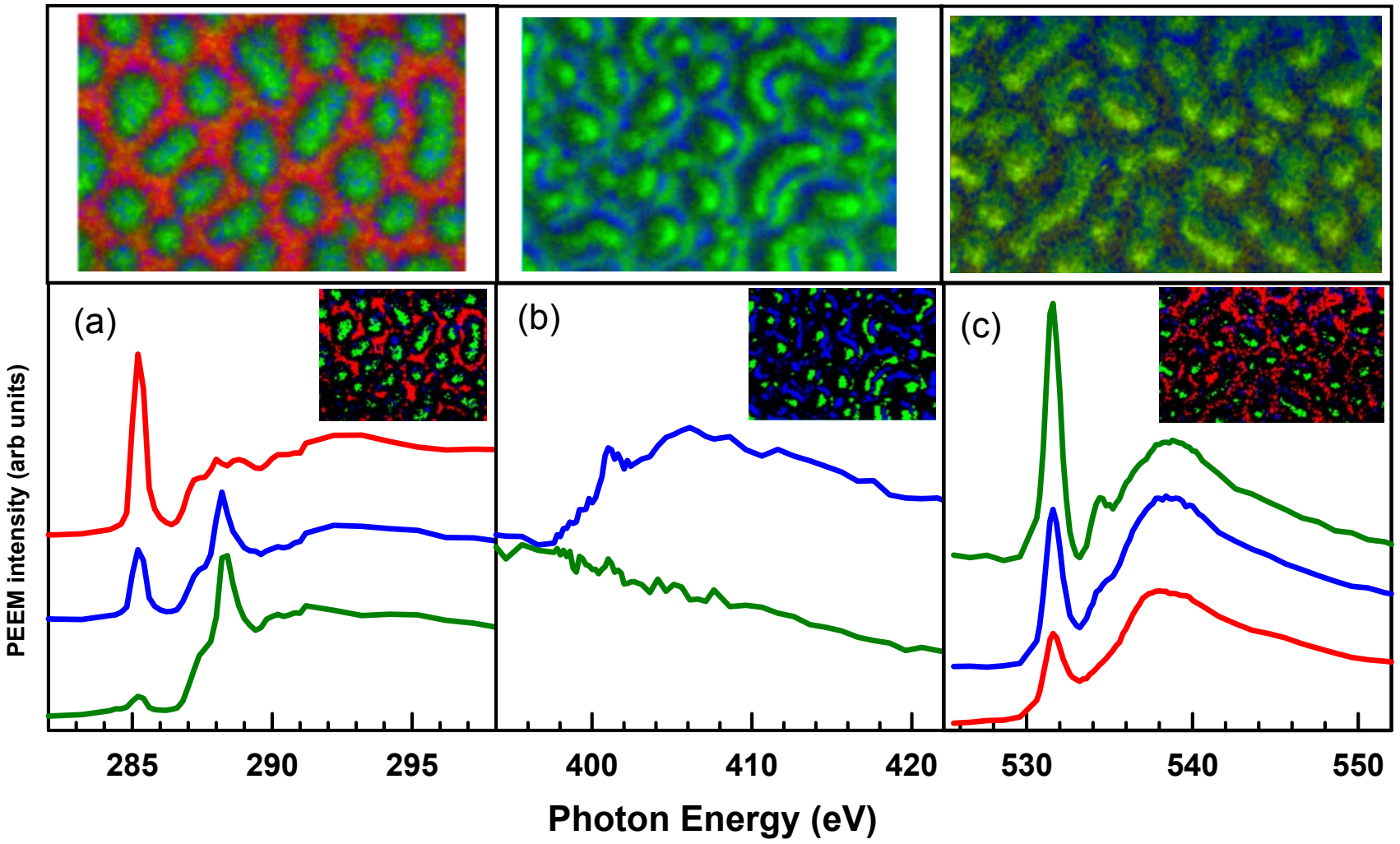
(a)
(b)
(c)
PEEM intensity (arb units)
285
290
295
400
410
420
530
540
550
Photon Energy (eV)

Fig 6